Available online at www.sciencedirect.com
SCIENCE DIRECT
Journal of Inorganic Biochemistry 93 (2003) 141–151
Journal of Inorganic Biochemistry
www.elsevier.com/locate/jinorgbio

Synthesis, equilibrium studies and structural characterisation of the Zn(II) complexes with trimethylene-N^6,$N^{6'}$-bisadenine

Ángel García-Raso[a,*], Juan J. Fiol[a], Ferran Bádenas[a], Andrés Tasada[a], Xavier Solans[b], Mercè Font-Bardia[b], Manuel G. Basallote[c], María A. Máñez[c], María J. Fernández-Trujillo[c], David Sánchez[c]

[a]*Departament de Química, Universitat de les Illes Balears, 07071 Palma de Mallorca, Spain*
[b]*Departament de Cristal·lografia, Mineralogia i Dipòsits Minerals, Universitat de Barcelona, 08028 Barcelona, Spain*
[c]*Departamento de Ciencia de los Materiales e Ingeniería Metalúrgica y Química Inorgánica, Universidad de Cádiz, Apdo. 40, Puerto Real, 11510 Cádiz, Spain*

Received 14 May 2002; received in revised form 21 August 2002; accepted 27 August 2002

Abstract

The new compound trimethylene-N^6,$N^{6'}$-bisadenine (L), in which two adenine molecules are linked together by a trimethylene bridge that connects the N^6 atoms, has been prepared. Reaction of L with $HgCl_2$ and $ZnCl_2$ in concentrated HCl solution leads to crystalline solids. The X-ray characterisation of the Hg(II) complex $(H_2L)[HgCl_4]\cdot 3H_2O$ reveals that it is an outer-sphere complex in which the ligand is protonated at N(1) and N(1′). In contrast, the structure of the complex $[H_2L(ZnCl_3)_2]\cdot 2H_2O$ shows the ligand co-ordinated to two different Zn(II) ions through the N(7) of both adenine fragments, the protons being located on the N(1) atoms. The latter compound constitutes the first crystallographic evidence of an inner sphere complex with bis-adenines and, for this reason, an equilibrium study was carried out on the Zn(II)-L-H^+ system. Potentiometric studies indicate that L is protonated in aqueous solution to form HL^+ and H_2L^{2+} with $\log K_H$ values of 4.42 and 3.35 (25 °C, 0.10 M KNO_3). The data from potentiometric titrations in the presence of Zn^{2+} can be analysed considering the formation of the species LZn^{2+}, $HLZn^{3+}$, LZn_2^{4+} and $HLZn_2^{5+}$, whose stability constants exceed the value expected for a monodentate interaction of the metal ion with adenine and suggest the possibility of a polydentate behaviour of L in the pH range 2.5–5.0. In contrast, spectrophotometric titrations carried out under conditions similar to those used in the synthetic work (1 M HCl) can be fitted with a model involving exclusively the H_2LZn^{4+} and $H_2LZn_2^{6+}$ species with $\log K_M$ values reasonable for the interaction of Zn(II) with the N(7) of the protonated adenine fragments. Despite the $H_2LZn_2^{6+}$ species has a low stability, the spectrophotometric results are in agreement with its formation under the conditions in which the solid complex was prepared.

Keywords: Zn(II) complexes; Trimethylene-N^6,$N^{6'}$-bisadenine; X-ray structures; Equilibrium studies

1. Introduction

Metal complexes with nucleotides, nucleosides and nitrogen bases have been a topic of great interest during the last years because of the important role of metal ions in the biochemistry of nucleic acids [1–3]. Since intrastrand crosslinks at adjacent purine bases are one of the preferred interactions between soft transition metal ions and DNA, good models of such interactions would involve dinucleotide analogues in which the bases are connected by a polymethylene chain [4]. Zinc is one of the most important metals in biological systems, being an integral component of more than 200 enzymes [5,6].

In previous papers [7,8] we described the synthesis and structural characterisation of Zn(II), Cd(II) and Hg(II) complexes of the model ligand trimethylene-9,9′-bisadenine. The three complexes yielded outer sphere structures in which both atoms N(1) and N(1′) from the ligand are protonated. The Zn(II) and Hg(II) complexes show the same type of anion (MCl_4^{2-}) and identical pattern of hydrogen bonds between the ligand and the anion [N(6)···Cl, N(6′)···Cl and N(1)···Cl]. On the other hand, the Cd(II) complex presents the dimeric $[Cd_2Cl_8(H_2O)_2]^{4-}$ anion and no H-bonds were found between the protonated trimethylene-bisadenine and the cadmium dimer.

In the present paper we report the synthesis of the new

---

*Corresponding author. Fax: +34-971-173-426.
E-mail address: dquagr0@clust.uib.es (Á. García-Raso).

0162-0134/02/$ – see front matter © 2002 Elsevier Science Inc. All rights reserved.
PII: S0162-0134(02)00568-8

ligand trimethylene-N^6,$N^{6'}$-bisadenine, $(AdeNH)_2C_3$ (L), in which the trimethylene chain is connected to the exocyclic amino groups of two adenine bases (N^6 and $N^{6'}$). Metal complexes of N^6-substituted adenines have been prepared and the biological activity of some of them has been also tested [9,10] but, to our knowledge, there is no previous report of metal complexes with N^6-substituted bis(adenines). Under conditions similar to those used with trimethylene-9,9′-bisadenine, we have prepared the $[H_2L(ZnCl_3)_2]\cdot 2H_2O$ complex, which is the first structurally characterised bis-adenine inner sphere complex and contains two Zn(II) ions bound to the N(7) and N(7′) atoms of the bis-adeninium ligand. A structurally characterised dimeric bis-hypoxanthine–Pt(II) compound in which each Pt(II) cation is co-ordinated to two hypoxanthine bases via N(7), has been previously reported [11]. In contrast, the reaction of L with $HgCl_2$ in acidic solution leads to the outer sphere complex $(H_2L)[HgCl_4]\cdot 3H_2O$. As the Zn(II) complex shows a singular behaviour between all the bis-adenine complexes that we have prepared to date, we decided to carry out an equilibrium study on the formation of the Zn(II)-L complexes and the results are also presented in the paper.

2. Experimental

2.1. Analysis and physical measurements

Elemental analyses were carried out using a Carlo-Erba model 1106 microanalyser. Infrared spectra (KBr pellets) were recorded on a PE 683 spectrophotometer with a PE 1600 infrared data station. Electronic spectra were obtained in aqueous solution on a PE 552 spectrophotometer. The potentiometric titrations were carried out with a Crison 2002 pH-meter provided with an Ingold combined electrode and calibrated to read pH as $-\log [H^+]$ by fitting the data corresponding to titrations of the HNO_3 solution with KOH. The spectrophotometric titrations were monitored in the 250–800 nm wavelength range with an Avantes PC2000 spectrophotometer. ^{1}H and ^{13}C NMR spectra were obtained with a Bruker AMX 300 spectrometer. Proton and carbon chemical shifts in dimethylsulfoxide (DMSO-d_6) were referenced to DMSO-d_6 [^{1}H NMR, δ(DMSO)$=2.60$; ^{13}C NMR, δ(DMSO)$=43.5$ ppm]. All organic (Sigma) and inorganic (Aldrich, Merck and Probus) reagents were used without further purification.

2.2. *Preparation of trimethylene-N^6,$N^{6'}$-bisadenine $(AdeNH)_2C_3$* ***(1)*** *and trimethylene-N^6,$N^{6'}$-bisadeninium dichloride $[(H\text{-}AdeNH)_2C_3]Cl_2$* ***(2)***

The preparation of the ligand was performed following a method previously described in the literature [12]. A suspension of 1 g (0.007 mol) of 6-chloropurine in 20 ml of 1-butanol and 3 ml of triethylamine was refluxed with 0.37 g (0.004 mols) of 1,3-propanediamine and a few drops of water during 3 h. The resulting solid was filtered off and washed with water and acetone. A more purified product could be obtained by treatment with 2 M NaOH and reprecipitated with acetic acid, yielding the final product (40–50%). Found: C, 41.2; H, 5.4; N, 36.5%. Calc. for $C_{13}H_{22}N_{10}O_4$ corresponding to $(AdeNH)_2C_3\cdot 4H_2O$: C, 40.8; H, 5.6; N, 36.7%. IR (cm^{-1}): 666s, 680m, 731w, 771w, 797m, 864m, 904s, 947s, 1056w, 1098m, 1143m, 1167m, 1268s, 1304vs, 1333s, 1364m, 1379m, 1406m, 1450m, 1471m, 1538w, 1608vs, 1623vs. ^{1}H NMR (DMSO-d_6): δ 12.98 bs [2H, H(9)/H(9′)], 8.30 s [2H, H(2)/H(2′)], 8.22 s [2H, H(8)/H(8′)], 7.92 bs [2H, H(10)/H(10′)], 3.66 bt [4H, C(11)-H_2/C(11′)-H_2], 2.00 t [4H, C(12)-H_2, $J=6.6$ Hz]. ^{13}C NMR (DMSO-d_6): d 158.7 [C(6)], 156.6 [C(2)], 153.5 [C(4)], 143.0 [C(8)], 122.9 [C(5)], 41.4 [C(11)], 33.4 [C(12)]. Dissolution of **1** in 1 M HCl yields the corresponding hydrochloride **2**. Found: C, 36.7; H, 4.7; N, 32.8%. Calc. for $C_{13}H_{21}Cl_2N_{10}O_{2.5}$ corresponding to $[(H\text{-}AdeNH)_2C_3]Cl_2\cdot 2.5H_2O$: C, 36.4; H, 4.9; N, 32.7%. IR (cm^{-1}): 486w, 530m, 555w, 630s, 655m, 671vw, 726vw, 781s, 869m, 888m, 943m, 987m, 1035w, 1047w, 1094vw, 1120vw, 1143m, 1168m, 1216s, 1290w, 1310vw, 1331w, 1380m, 1414s, 1440m, 1469vw, 1511m, 1602s, 1678vs. ^{1}H NMR (DMSO-d_6): d 9.92 bs [2H, N(9)/H(9′)], 8.66 s [2H, H(2)/H(2′)], 8.64 s [2H, H(8)/H(8′)], 3.84 bt [4H, C(11)-H_2/C(11′)-H_2], 2.17 t [4H, C(12)-H_2, $J=6.7$ Hz].

2.3. *Preparation of $[(H\text{-}AdeNH)_2C_3](HgCl_4)\times 3H_20$* ***(3)***

To a stirred warm (50 °C) solution of 0.38 g (0.001 mols) of **1** in 25 ml of 1 M HCl, 0.002 mols of $HgCl_2$ were added. The resulting solution was kept to 50 °C during 30 min and then was allowed to stay at room temperature. The precipitated complex was filtered off, washed with water and acetone and air-dried (40–45%). After a week, in the filtered solution, crystals of **3** suitable for X-ray diffraction were formed. Found: C, 21.9; H, 3.2; N, 19.6%. Calc. for $C_{13}H_{22}Cl_4HgN_{10}O_3$ corresponding to $[(H\text{-}AdeNH)_2C_3](HgCl_4)\cdot 3H_2O$: C, 22.0; H, 3.1; N, 19.7%. IR (cm^{-1}): 311m, 347vw, 476w, 499vw, 518w, 541s, 610s, 611w, 693vw, 725w, 748m, 776s, 886w, 899m, 926w, 967vw, 1029vw, 1083w, 1121m, 1149m, 1201s, 1297m, 1347s, 1397s, 1427s, 1462m, 1485w, 1515m, 1644vs, 1662vs. ^{1}H NMR (DMSO-d_6): d 9.63 bs [2H, N(9)/H(9′)], 8.66 s [2H, H(2)/H(2′)], 8.62 s [2H, H(8)/H(8′)], 3.81 bt [4H, C(11)-H_2/C(11′)-H_2], 2.17 t [4H, C(12)-H_2, $J=6.3$ Hz]. $\Lambda_M(\Omega^{-1}\ cm^2\ mol^{-1})$ of 10^{-3} M in DMSO, 20 °C=52.

2.4. *Preparation of $\{[(H\text{-}AdeNH)_2C_3](ZnCl_3)_2\}\cdot 2H_2O$* ***(4)***

To a stirred warm (50 °C) solution of 0.38 g (0.001 mols) of **1** in 25 ml of 1 M HCl, 0.012 mols of $ZnCl_2$

dissolved in 25 ml of 1 M HCl were added. The resulting solution was kept to 50 °C during 30 min and then it was allowed to stay at room temperature. The crystalline complex was filtered off, washed with water and acetone and air-dried (80%). After a week, crystals of **4** suitable for X-ray diffraction were formed from the filtrate. Found: C, 22.6; H, 2.9; N, 20.1%. Calc. for $C_{13}H_{20}Cl_6N_{10}O_2Zn_2$ corresponding to $\{[(\text{H-AdeNH})_2C_3](ZnCl_3)_2\}\cdot 2H_2O$: C, 22.5; H, 2.9; N, 20.2%. IR (cm^{-1}): 314s, 357vw, 487m, 541m, 551m, 587m, 639m, 664m, 762m, 781m, 838m, 907m, 976s, 1079w, 1105vw, 1126m, 1135m, 1162vw, 1225s, 1298w, 1354s, 1370m, 1405m, 1420m, 1435w, 1468s, 1532w, 1605vs, 1621vs, 1673vs, 1682vs. ^{1}H NMR (DMSO-d_6): d 9.57 bs [2H, N(9)/H(9′)], 8.66 s [2H, H(2)/H(2′)], 8.61 s [2H, H(8)/H(8′)], 3.81 bt [4H, C(11)-H_2/C(11′)-H_2], 2.17 t [4H, C(12)-H_2, J=6.6 Hz]. Λ_M(Ω^{-1} cm^2 mol^{-1}) of 10^{-3} M in DMSO, 20 °C=23.

2.5. Crystallographic studies

Prismatic crystal (0.1×0.1×0.2 mm) were selected and mounted on an Enraf-Nonius CAD4 four-circle diffractometer. Unit-cell parameters were determined from automatic centring of 25 reflections ($12<\theta<21°$) and refined by least-squares method. Intensities were collected with graphite monochromatized Mo Kα radiation, using $\omega/2\theta$ scan-technique. Three reflections were measured every 2 h as orientation and intensity control, significant intensity decay was not observed. Lorentz-polarization but not absorption corrections were made. The structures were solved by Direct methods, using SHELXS [13] computer program and refined by full-matrix least-squares method with SHELX-93 computer program [14]. Selected crystallographic data are presented in Table 1.

Compound **3**: The function minimised was $\Sigma\omega\|F_o|^2-|F_c|^2|^2$, where $\omega=[\sigma^2(I)+(0.0516P)^2]^{-1}$, and $P=(|F_o|^2+2|F_c|^2)/3$, f, f' and f'' were taken from International Tables of X-ray Crystallography [15]. Nineteen H atoms were located from a difference synthesis and refined with an overall isotropic temperature factor and 15 H atoms were computed and refined with an overall isotropic temperature factor using a riding model.

Compound **4**: The function minimised was $\Sigma\omega\ \|F_o|^2-|F_c|^2|^2$, where $\omega=[\sigma^2(I)+(0.0591P)^2+2.5371\,P]^{-1}$, and $P=(|F_o|^2+2|F_c|^2)/3$, f, f' and f'' were taken from International Tables of X-ray Crystallography [15]. The extinction coefficient was 0.0048(3). All H atoms were located from a difference synthesis and refined with an overall isotropic temperature factor.

Table 1
Selected crystallographic data for $[(\text{H-AdeNH})_2(CH_2)_3](HgCl_4)\cdot 3H_2O$ **3** and $\{[\text{H-AdeNH})_2(CH_2)_3](ZnCl_3)_2\}\cdot 2H_2O$ **4**

Crystal data	**3**	**4**
Empirical formula	$C_{13}H_{22}Cl_4HgN_{10}O_3$	$C_{13}H_{20}Cl_6N_{10}O_2Zn_2$
Crystal size (mm)	0.1×0.1×0.2	0.1×0.1×0.2
Crystal system	Triclinic	Monoclinic
Space group	*P-1*	*C2/c*
Unit cell dimensions	a=7.710(5) Å	a=10.465(4) Å
	b=12.388(3) Å	b=12.522(4) Å
	c=24.396(3) Å	c=19.443(15) Å
	α=85.49(2)°	
	β=89.46(4)°	β=96.07(5)°
	γ=83.39(3)°	
Volume (Å^3)	2307.4(18)	2534(2)
Z	4	4
Formula weight	708.80	691.83
Density (calc.) (mg/m^3)	2.040	1.814
Absorption coefficient (mm^{-1})	7.171	2.559
F(000)	1368	1384
Data collection and refinement		
θ range (°)	2.26 to 29.97	2.11 to 30.04
Index ranges	$-10\leq h\leq 10$	$-14\leq h\leq 14$
	$-17\leq k\leq 17$	$0\leq k\leq 17$
	$0\leq l\leq 34$	$0\leq l\leq 27$
Reflections collected	13413	3784
Independent reflections	13413 [R(int)=0.0087]	3663 [R(int)=0.0308]
Data/restraints/parameters	13413/0/622	3663/0/192
Final R indices [$I>2\sigma(I)$]	$R1$=0.0319	$R1$=0.0352
	$wR2$=0.0756	$wR2$=0.0932
R indices (all data)	$R1$=0.0801	$R1$=0.0401
	$wR2$=0.0960	$wR2$=0.0971
Goodness-of-fit on F^2	0.954	1.106
Largest difference peak (eÅ^{-3})	0.833	0.856
Largest difference hole (eÅ^{-3})	−0.939	−0.869

2.6. Equilibrium measurements

The stock solutions of KOH, $Zn(NO_3)_2 \cdot 6H_2O$ and HNO_3 required for the potentiometric determinations of equilibrium constants were prepared at concentrations close to 0.10 M. The KOH solution was titrated with potassium hydrogen phthalate (phenolphthalein indicator) and was then used to titrate the HNO_3 solution with the same indicator. The Zn(II) solution was titrated with EDTA (erioT indicator). Potentiometric titrations were carried out at 25.0±0.1 °C under a N_2 atmosphere in the presence of 0.10 M KNO_3 as supporting electrolyte. Solutions of the ligand (40.0 ml) with an initial concentration close to 1.5×10^{-3} M were prepared in water containing the supporting electrolyte, and the required amounts of the HNO_3 and Zn(II) solutions were then added before titration with KOH.

The protonation constants of the ligand were obtained from two titrations of the ligand alone and the reported equilibrium constants correspond to the mean value and standard deviation of the values derived from both titrations. The data corresponding to titration of solutions containing Zn(II) and L in 2:1 and 1:1 molar ratios were then analysed to obtain the equilibrium constants for the formation of Zn(II)-L complexes, the reported values corresponding now to the mean value and standard deviation of the values derived from both titrations. In all cases the titrations had to be interrupted at relatively low pH (ca. 4.8) because of precipitation. The number of points measured was different for every titration and ranges from 38 to 60, covering a pH range from 2.7 to 4.8. The analysis of the data was carried out with program BEST and the species distribution curves were obtained with programs SPE and SPEPLOT [16]. During all refinements the value of $\log K_w$ was fixed at –13.78. For titrations containing Zn(II) and L, the formation constants corresponding to the protonated forms of the ligand were fixed at the values derived from titrations of the ligand alone. The Zn(II)-OH^- complexes were also introduced in the model with formation constants fixed at their corresponding literature values [17], although their effect is negligible because they are not formed at significant extent at the pH achieved in the presence of the ligand.

For the spectrophotometric titrations, solutions of L in 1.0 M HCl were prepared ($[L]_0 = 1.8$–4.1×10^{-5} M) and titrated with solutions of Zn(II) previously titrated with EDTA. Two sets of titrations were carried out using different sources and concentrations of Zn(II) ions; for the first set a 0.2 M solution of $ZnCl_2$ was used, whereas a 1.0 M solution of $ZnSO_4 \cdot 7H_2O$ was used for the second one. Although the use of HNO_3 and/or $Zn(NO_3)_2$ would make the results more comparable with those derived from potentiometric titrations, the presence of the nitrate ion was avoided because its absorption band interferes with the spectral changes associated to the formation of Zn-L complexes. Because of the low stability of the Zn(II)-L complexes, high concentrations of Zn(II) were required in order to achieve a significant degree of complex formation and so, 35–50 spectra were recorded for each titration covering a [Zn(II)] range of ca. 0–0.1 M ($ZnCl_2$ solutions) or 0–0.4 M ($ZnSO_4$ solutions). Although in the latter case there are significant changes in $[H^+]$ during the titrations that probably increase the error in the estimated values of the equilibrium constants, the results were considered more reliable than if only the first part of the titrations, in which $[H^+]$ can be considered to remain constant, were considered.

As the $H_2LZn_2^{6+}$ species had been isolated as a solid complex and the potentiometric results had shown that L exists as H_2L^{2+} in acidic solutions, the spectrophotometric data were fitted with Eq. (1) [18] to an equilibrium model that assumes the formation of the H_2LZn^{4+} and $H_2LZn_2^{6+}$ species. In Eq. (1), ΔAbs represents the experimental absorbance change of Zn(II) containing solutions with respect to analogous solutions without added Zn(II), $[H_2L^{2+}]_0$ is the total concentration of protonated ligand, K_{M1} is the equilibrium constant for the formation of the 1:1 (H_2L^{2+}:Zn) complex and $\Delta\varepsilon_1$ is the change in the molar absorptivity of the 1:1 complex with respect to the ligand. Analogously, K_{M2} and $\Delta\varepsilon_2$ represent the stability constant and the change in the molar absorptivity of the 1:2 complex. Because of the large excess of Zn(II), the values of [Zn(II)] in Eq. (1) coincide with the total concentration of Zn(II) added at each titration point. The reported values of the stability constants correspond to the mean value and standard deviation of the values derived from three titrations. The data were also analysed assuming an equilibrium model that only considers the formation of the 1:1 complex; in that case, the analysis was made using a simplified form of Eq. (1) in which the terms containing K_{M2} are ignored.

$$\frac{\Delta\text{Abs}}{[H_2L^{2+}]_0} = \frac{K_{M1}\Delta\varepsilon_1[\text{Zn(II)}] + K_{M1}K_{M2}\Delta\varepsilon_2[\text{Zn(II)}]^2}{1 + K_{M1}[\text{Zn(II)}] + K_{M1}K_{M2}[\text{Zn(II)}]^2} \tag{1}$$

3. Results

*3.1. The crystal structure of $[(H\text{-}AdeNH)_2C_3](HgCl_4)\cdot 3H_2O$ (**3**) and $\{[(H\text{-}AdeNH)_2C_3](ZnCl_3)_2\}\cdot 2H_2O$ (**4**)*

Information related to the protonation sites of the trimethylene-N^6,$N^{6'}$-bisadenine ligand was obtained from the isolation of the outer sphere complex **3**. Chloride, nitrate and perchlorate salts of H_2L^{2+} were obtained only as microcrystalline samples. However, utilisation of $[HgCl_4]^{2-}$ yielded crystals suitable for X-ray crystallography. The Hg(II) complex contains two different units labelled Unit 1 and Unit 2 in Fig. 1. Each unit is constituted by a ligand molecule di-protonated in N(1) and

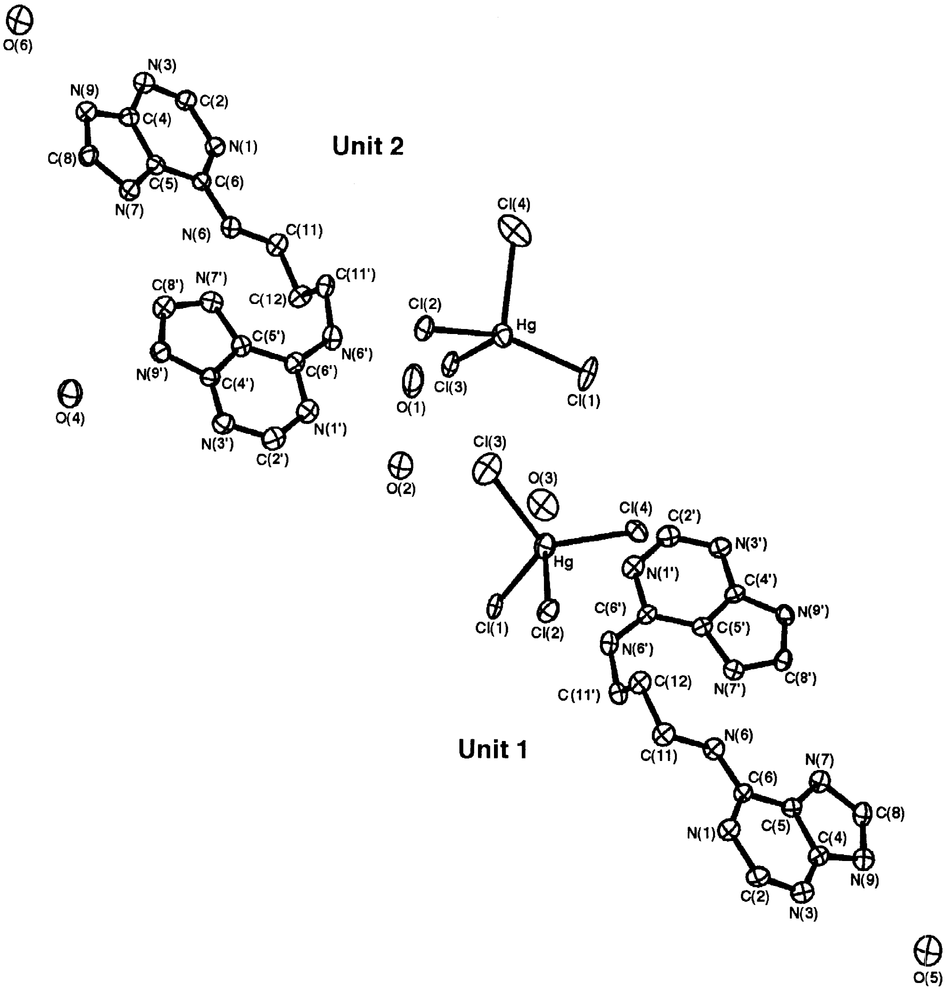

Fig. 1. ORTEP plot of $[(H\text{-}AdeNH)_2C_3](HgCl_4)\cdot 3H_2O$ **3**. Hydrogen atoms have been omitted for clarity.

N(1′), and a distorted $[HgCl_4]^{2-}$ anion. An intramolecular interaction between N(6) and N(7′) [N(6)···N(7′) ca. 3 Å] determines an approach between the two adeninium rings. Moreover, the two tetrahalomercuriate ions are very different, the Hg–Cl distances being in the range of 2.4149(17) and 2.5654(14) Å for Unit 1, and in the range of 2.3678(14) and 2.7101(17) Å for Unit 2 (Table 2). The later shows a very large Hg–Cl length, of 2.7101(17) Å, as compared with other distances of related complexes described in the literature [19–21]; moreover, the $[HgCl_4]^{2-}$ anion of Unit 1 is very similar to that reported for the trimethylene-9,9′-bisadeninium mercury complex [8]. The two chloromercuriate ions exhibit an additional hydrogen bond with the ligand molecule [N(6)···Cl = 3.21 and 3.22 Å in Units 1 and 2, respectively].

The crystal structure of complex **4** is shown in Fig. 2 and selected bond distances and angles are given in Table 2. The complex shows an inner sphere structure where the ligand is co-ordinated, via N(7) and N(7′), to two different zinc atoms. Three chloride ions complete the co-ordination sphere around the metal, which presents tetrahedral hybridisation. The two $[ZnCl_3(N^6\text{-alkyl-adeninium})]$ moieties, protonated at the N(1) atom, are related by a 2-fold axis. Although co-ordination to metal ions through the N(7) atom is common for adenosine and other 9-substituted adenines, the availability of the N(9) site for metal coordination is well established for adenine. Actually, metal complexes are known in which the metal ion is coordinated to the N(9) site of neutral adenine and its protonated and deprotonated forms [22]. However, it is important to note that one of the few well documented cases in which N(9) does not participate in metal binding is $(HL')ZnCl_3$ (L′ = adenine), which contains Zn(II) coordinated at N(7) [23].

The structure of compound **4** shows similar characteristics to Zn(II) complexes with 9-alkyladenines described in the literature [24–27] (there is a lack of structural information regarding zinc complexes of N^6-alkyladenines); thus (i) presents similar bond distances around the zinc atom, [Zn-N(7) = 2.0732(19), Zn-Cl(1) = 2.2544(16), Zn-Cl(2) = 2.2376(11) and Zn-Cl(3) = 2.2369(9) Å]; (ii) the zinc atom presents an important deviation of the planarity with respect to the imidazole ring τ[Zn-N(7)-C(8)-N(9) = 160.60 °]; (iii) one chlorine atom is involved in a hydrogen

Table 2
Selected bonds (Å) and angles (°) for complexes **3** and **4**

	Zn(II) inner sphere complex **4**	Hg(II) outer sphere complex **3**	
Zn–N(7)	2.0732(19)		
M–Cl(1)	2.2544(16)	2.5648(14)	2.7101(17)
M–Cl(2)	2.2376(11)	2.5190(19)	2.633(2)
M–Cl(3)	2.2396(9)	2.4149(17)	2.3678(14)
Hg–Cl(4)		2.4228(14)	2.3778(14)
N(1)–C(2)	1.366(2)	1.367(6)	1.367(6)
N(1′)–C(2′)		1.362(6)	1.339(6)
C(2)–N(3)	1.297(3)	1.285(6)	1.271(6)
C(2′)–N(3′)		1.308(6)	1.328(6)
N(3)–C(4)	1.354(2)	1.367(6)	1.375(5)
N(3′)–C(4′)		1.349(5)	1.357(6)
C(4)–C(5)	1.382(2)	1.384(5)	1.388(6)
C(4′)–C(5′)		1.387(6)	1.383(6)
C(5)–C(6)	1.407(2)	1.416(6)	1.385(6)
C(5′)–C(6′)		1.398(6)	1.400(6)
N(1)–C(6)	1.361(2)	1.359(5)	1.354(5)
N(1′)–C(6′)		1.370(5)	1.378(6)
C(6)–N(6)	1.316(2)	1.305(5)	1.333(5)
C(6′)–N(6′)		1.314(6)	1.313(6)
C(5)–N(7)	1.381(2)	1.361(5)	1.384(5)
C(5′)–N(7′)		1.399(5)	1.395(5)
N(7)–C(8)	1.325(2)	1.326(6)	1.327(6)
N(7′)–C(8′)		1.318(5)	1.290(6)
C(8)–N(9)	1.348(3)	1.342(6)	1.360(6)
C(8′)–N(9′)		1.345(6)	1.372(6)
C(4)–N(9)	1.362(2)	1.350(6)	1.341(5)
C(4′)–N(9′)		1.343(6)	1.360(6)
N(6)–C(10)	1.465(2)	1.477(5)	1.431(6)
N(6′)–C(10′)		1.442(6)	1.462(6)
C(10)–C(11)	1.520(2)	1.521(6)	1.520(6)
C(11)–C(10′)	1.520(2)#1	1.512(7)	1.529(6)
N(7)–Zn–Cl(1)	100.31(7)		
N(7)–Zn–Cl(2)	100.93(6)		
N(7)–Zn–Cl(3)	109.70(5)		
Cl(1)–M–Cl(2)	119.55(4)	100.11(6)	96.75(7)
Cl(1)–M–Cl(3)	109.94(3)	107.57(6)	97.99(5)
Cl(2)–M–Cl(3)	114.56(3)	108.32(6)	103.20(7)
Cl(1)–Hg–Cl(4)		107.20(5)	96.24(5)
Cl(2)–Hg–Cl(4)		111.29(5)	99.01(6)
Cl(3)–Hg–Cl(4)		120.36(7)	151.90(5)
C(8)–N(7)–Zn	104.73(15)		
C(5)–N(7)–Zn	131.51(12)		
N(1)–C(2)–N(3)	126.16(19)	125.6(4)	126.6(4)
N(1′)–C(2′)–N(3′)		124.6(4)	125.5(5)
C(2)–N(3)–C(4)	112.66(16)	112.1(4)	111.9(4)
C(2′)–N(3′)–C(4′)		111.8(4)	110.0(4)
N(3)–C(4)–C(5)	126.71(17)	127.3(4)	125.8(4)
N(3′)–C(4′)–C(5′)		127.7(4)	129.3(4)
C(4)–C(5)–C(6)	118.38(17)	117.6(4)	118.8(4)
C(4′)–C(5′)–C(6′)		118.5(4)	117.5(4)
C(5)–C(6)–N(1)	113.55(16)	113.5(4)	114.1(4)
C(5′)–C(6′)–N(1′)		112.5(4)	112.9(4)
C(6)–N(1)–C(2)	123.48(17)	123.9(4)	122.7(4)
C(6′)–N(1′)–C(2′)		124.7(4)	124.7(4)
N(6)–C(6)–N(1)	120.93(17)	121.3(4)	120.6(4)
N(6′)–C(6′)–N(1′)		119.5(4)	119.9(4)
N(6)–C(6)–C(5)	125.52(17)	125.2(4)	125.3(4)
N(6′)–C(6′)–C(5′)		128.0(4)	127.1(4)
C(5)–N(7)–C(8)	104.73(15)	103.1(4)	103.1(4)
C(5′)–N(7′)–C(8′)		104.1(3)	104.0(4)
N(7)–C(8)–N(9)	112.43(17)	113.5(4)	113.3(4)
N(7′)–C(8′)–N(9′)		112.4(4)	113.3(4)

Table 2. Continued

	Zn(II) inner sphere complex **4**	Hg(II) outer sphere complex **3**	
C(8)–N(9)–C(4)	107.17(16)	107.0(4)	107.0(4)
C(8′)–N(9′)–C(4′)		108.6(4)	107.1(4)
N(9)–C(4)–C(5)	106.09(16)	105.2(4)	106.1(4)
N(9′)–C(4′)–C(5′)		105.4(4)	104.9(4)
C(4)–C(5)–N(7)	109.58(16)	111.3(4)	110.6(4)
C(4′)–C(5′)–N(7′)		109.5(4)	110.7(4)
N(3)–C(4)–N(9)	127.19(17)	127.6(4)	128.2(4)
N(3′)–C(4′)–N(9′)		126.8(4)	125.9(4)
C(6)–C(5)–N(7)	132.01(16)	131.1(4)	130.6(4)
C(6′)–C(5′)–N(7′)		131.9(4)	131.8(4)
C(6)–N(6)–C(10)	122.94(16)	123.7(4)	125.1(4)
C(6′)–N(6′)–C(10′)		125.2(4)	126.9(4)
N(6)–C(10)–C(11)	111.76(14)	107.9(4)	109.8(4)
N(6′)–C(10′)–C(11)		113.3(4)	110.2(4)
C(10)–C(11)–C(10′)	116.2(2)#1	112.5(4)	110.9(4)

Symmetry transformations used to generate equivalent atoms. #1 for **1**: $-x+2, y, -z+1/2$.

bond with the N(6)-H group [N(6)···Cl = 3.350(3) Å]; and (iv) the distance and angle values of the adenine moieties fit well in other N(1) protonated adenines. The crystallographic structure is completed by means of a couple of hydrogen bonds N(9)···N(3)#1 and N(3)···N(9)#1 [N(9)···N(3)#1 = 2.926(3) Å] between two adjacent units and completed with other Cl···OH_2 interactions.

3.2. IR spectra

Tentative assignments [28–30] of the IR spectra of all compounds are presented in Table 3. The most relevant features are: (i) shift to higher frequencies of the strong band at 1660 cm^{-1} in **1**, assigned to δ[NHR] (1678 cm^{-1} for **2**, 1682 cm^{-1} for **4**); and (ii) modification of the band at 1420 cm^{-1} in free ligand, related to the vibration ν[N(1)-C(6)-N(6)] (1423, 1405 cm^{-1} for **4**) possibly due to the implication of the N(1) atom in intramolecular hydrogen bonds.

3.3. Equilibrium determinations

The data from titration of L in the presence of added acid could be well fitted assuming a model with two protonation steps leading to the HL^+ and H_2L^{2+} species, whose formation constants are included in Table 4. The values of $\log K_H$ are very close to those previously reported for adenine [17,22,31–34], which indicates that alkyl substitution at the N(6) atom does not cause important changes in the basicity of the adenine fragments. The species distribution curves in Fig. 3 show that the major species at low pH is H_2L^{2+}, whereas the un-

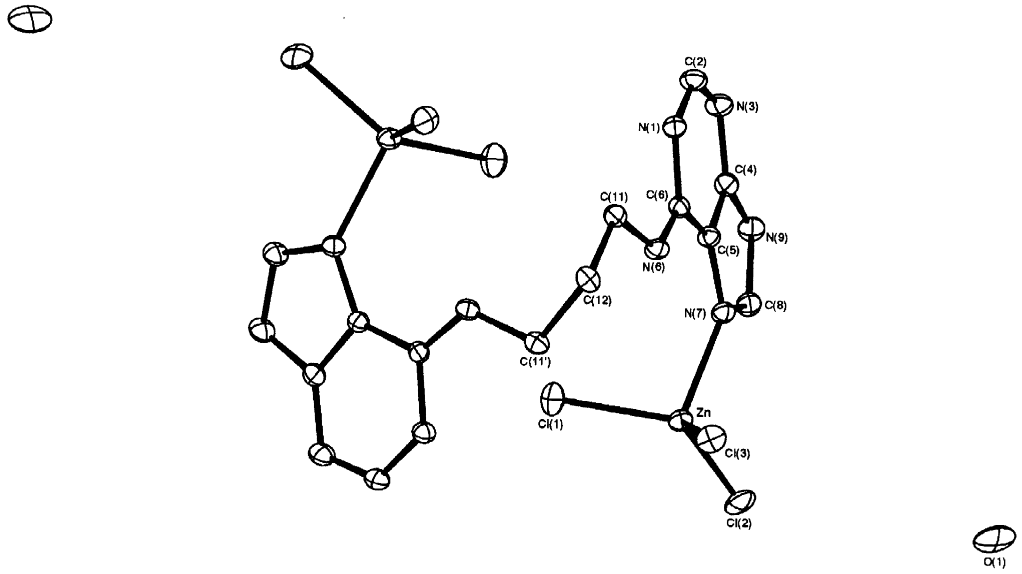

Fig. 2. ORTEP plot of {$[(H\text{-}AdeNH)_2C_3](ZnCl_3)_2$}·$2H_2O$ **4**. Hydrogen atoms have been omitted for clarity.

Table 3
Tentative assignation for compounds **1**–**4**

	$(AdeNH)_2C_3$ **1**	$(H\text{-}AdeNH)_2C_3$ **2**	$Hg\text{-}(AdeNH)_2C_3$ **3**	$Zn\text{-}(H\text{-}AdeNH)_2C_3$ **4**
δ[NHR]	1623	1678	1662	1682
δ[NHR] + ν[C(5)–C(6)]	1608	1602	–	1603
ν[C(4)–N(9)] + δ[C(8)–H] + δ[CH_2]	–	1511	1515	–
ν[C(4)–N(9)] + ν[C(5)–C(6)]	1471	1469	1462	1468
δ[C(2)–H] + ν[C(8)–N(9)] + δ[C(8)–H]	1450	1440	–	1435
ν[N(1)–C(6)–N(10)]	1420	1414	1423,1405	1427
ν(pyrimidine ring)	–	1380	1370	–
ν[C(5)–N(7)–C(8)]	1334	1331	–	–
ν[C(2)–N(3)] + ν[C(8)–N(9)] + δ[C–H]	1304	1301	1298	1297
δ[C(9)–H] + ring mode	1268	–	–	–

protonated form becomes the major species only at pH higher than 4.5.

The titrations of L in the presence of Zn(II) show significant differences with respect to those of the ligand alone, which indicates the formation of stable Zn(II)-L complexes in acidic solutions. A satisfactory fit of the potentiometric data was obtained with an equilibrium model that includes the species LZn^{2+}, $HLZn^{3+}$, LZn_2^{4+} and $HLZn_2^{5+}$, whose stability constants are included in Table 4. No significant improvement in the quality of the fit was achieved by adding species as H_2LZn^{4+} or $H_2LZn_2^{6+}$. The species distribution curves in Fig. 4 show that almost all the ligand is co-ordinated to Zn(II) between pH 2 and 5 in solutions containing a 2:1 molar ratio of Zn:L.

Although these results could explain the isolation of the $H_2LZn_2^{6+}$ complex at very low pH, where a second protonation of $HLZn_2^{5+}$ is reasonably expected to occur, we were surprised of the high stability of the LZn^{2+} and LZn_2^{4+} species. The equilibrium constants in Table 4 indicate that the stability constant for co-ordination of the first metal ion to the L and HL^+ species is higher than 4 (log units), whereas the values for co-ordination of the second Zn(II) are reduced by ca. 1 log unit, as expected

Table 4
Equilibrium constants derived from the analysis of potentiometric data for the protonation of L and for the formation of Zn(II)-L complexes in aqueous solution (25.0 °C, 0.10 M KNO_3, N_2 atmosphere)

Species	log β	Equilibrium	log K
Ligand protonation:			
HL^+	4.42(2)	$L + H^+/HL^+$	4.42
H_2L^{2+}	7.77(3)	$HL^+ + H^+/H_2L^{2+}$	3.35
Formation of Zn(II) complexes:			
LZn^{2+}	4.2(1)	$L + Zn^{2+}/LZn^{2+}$	4.2
LZn_2^{4+}	7.4(2)	$LZn^{2+} + Zn^{2+}/LZn_2^{4+}$	3.2
$HLZn^{3+}$	8.4(1)	$LZn^{2+} + H^+/HLZn^{3+}$	4.2
$HLZn_2^{5+}$	11.7(2)	$LZn_2^{4+} + H^+/HLZn_2^{5+}$	4.3
		$HL^+ + Zn^{2+}/HLZn^{3+}$	4.0
		$HLZn^{3+} + Zn^{2+}/HLZn_2^{5+}$	3.3

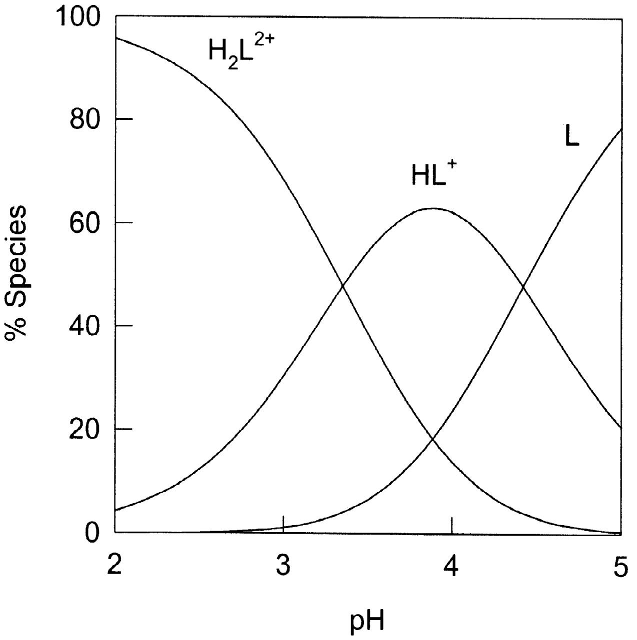

Fig. 3. Species distribution curves for solutions containing L at different pH values. The percentages are referred to the total concentration of the ligand.

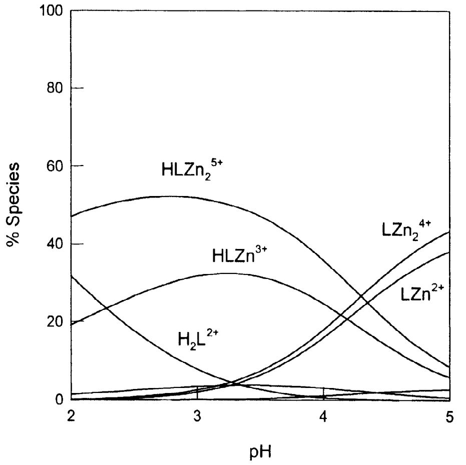

Fig. 4. Species distribution curves for solutions containing L and Zn(II) in 1:2 molar ratio. The percentages are referred to the total concentration of the ligand.

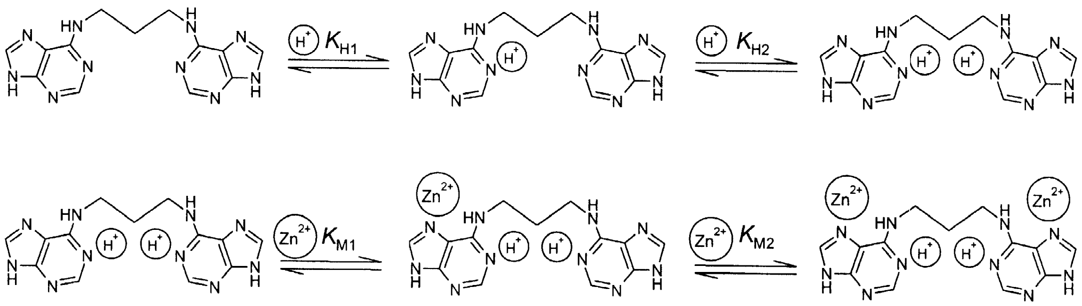

Fig. 5. Equilibrium model for the protonation of L and the formation of Zn(II) complexes in acidic solutions.

from electrostatic and statistical considerations. The log K_M values previously reported for the formation of the Zn(adenine)$^{2+}$ complex are usually below 2.5 [17,32], although a value as high as 8.28 has been also reported [33]. A value of log K_M smaller than 2 is also estimated for the interaction of Zn(II) with the N(7) of adenine from consideration of the well-established correlation of the log K_M versus log K_H data [35,36], which makes the value of log β for the L-Zn(II) complexes about two log units higher than expected for the monodentate interaction of the Zn(II) ions with the N(7) atoms of both adenine fragments. The data in Table 4 also indicate that the co-ordination of one or two Zn(II) ions only causes a small decrease of the first protonation constant of the ligand, which suggests that the N(1) sites are not involved in metal co-ordination.

The high stability of the L-Zn(II) and HL^{+}-Zn(II) species cannot be explained by an increased basicity of the ligand because the log K_H values of L and adenine are very close. The participation of the N^6 atoms in the interaction with the metal ion through hydrogen bonding to co-ordinated water (or chloride, as observed for **4**) could explain a certain stabilisation but the difference is too high to be explained in terms of this interaction. Because the titrations were carried out in 0.10 M KNO_3 and complex **4** was isolated from concentrated HCl solution, there is the possibility of changes in the co-ordination mode of L caused by a different degree of protonation, which could favour co-ordination through a different donor atom as N(9) or N(3) at higher pH. On the other hand, the presence-absence of high Cl^- concentrations in the synthetic procedure favours the existence of co-ordinated chlorides. However, these possible changes can hardly explain the large stability constant derived for the L-Zn(II) species. The possibility of a bidentate co-ordination of each adenine fragment to each Zn(II) ion cannot be excluded but this kind of interaction is not usual in adenine and substituted adenines. A possible explanation is to consider the interaction of each Zn(II) ion with the N(7) of one adenine and a different donor atom in the adjacent adenine within the same L molecule, which would lead to a bidentate interaction of L with both metal ions. This possibility is supported by previous reports showing the formation of dimeric or oligomeric species in which adenine (or its protonated and deprotonated forms), adenosine or N^6-substituted adenines act as a bridge between metal ions [9,10,32,37–40]. In any case, the equilibrium data do not provide unequivocal evidence on the existence of this kind of interaction and further work is clearly required to determine the coordination behaviour of L under the experimental conditions in which the potentiometric titrations are carried out.

Additional information about the stability of the Zn(II)-L complexes was obtained by carrying out spectrophotometric titrations under conditions similar to those used in the synthetic work. From the protonation constants of the ligand, the major species in 1.0 M HCl solutions is H_2L^{2+} and titration with Zn(II) under these conditions should lead to the sequential co-ordination of two metal ions according to the equilibrium scheme depicted in Fig. 5. Other possible equilibria leading to species different from those included in the figure are not shown because their concentrations must be negligible under these strongly acidic conditions. The possibility of higher protonated forms of the ligand can be excluded because complex **3** was isolated under similar experimental conditions and shows a single protonation at each adenine fragment. This conclusion is also supported by the lack of changes in the absorption spectra of L during titration with HCl in the concentration range from 10^{-2} to 1.0 M.

The titrations in the presence of metal ion showed that addition of Zn(II) causes changes in the absorption band of the ligand, the largest changes occurring at 260–270 nm. Fig. 6 shows a plot of these changes and the solid line represents the least-squares fit of the data by Eq. (1), which corresponds to an equilibrium model that assumes the formation of 1:1 and 1:2 complexes between H_2L^{2+} and Zn(II). The log K_M values so derived for the H_2LZn^{4+} and $H_2LZn_2^{6+}$ species in 1.0 M HCl are 1.6±0.1 and 1.2±0.1, respectively, when $ZnCl_2$ is used as the source of Zn(II) ions. Slightly different values of log K_M (0.9±0.1 and 0.1±0.3) are obtained when the titrations are carried out using solutions of $ZnSO_4$. In the latter case, the log K_{M2} value is not well defined by the experimental data and a satisfactory fit is also obtained when the $H_2LZn_2^{6+}$ species is ignored, the value derived for log K_{M1} being 0.7±0.1 in that case.

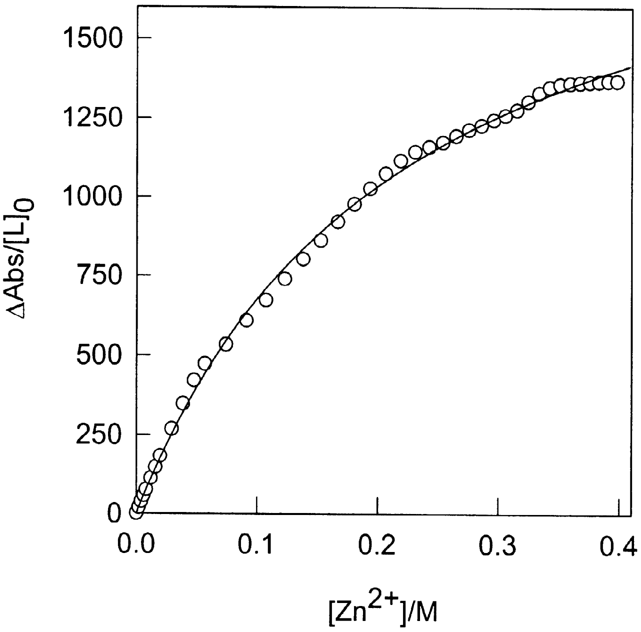

Fig. 6. Plot of the absorbance changes at 260 nm during titration of L with a solution of Zn(II) prepared from $ZnSO_4$. The solid line corresponds to the fit of experimental data by Eq. (1) in the text.

The differences between the values derived from both sets of titrations are surely caused by some interaction of the sulphate anions with the metal ions at the high concentrations of salt achieved during the titrations; actually the stability of the 1:1 complex of Zn(II) with HSO_4^- ($\log K = 0.89$) is higher than that with Cl^- ($\log K = 0.0$) [17] and it is expected that the presence of large concentrations of sulphate decrease the stability of the Zn(II)-L complexes. In any case, both sets of values are smaller than those previously reported for the interaction of Zn(II) with N(7) of adenine (ca. 2.0) and they appear reasonable when the de-stabilising effect of the positive charges are considered. Actually, a decrease of ca. 1 log unit is observed in the stability of the protonated adenosine complexes with respect to the analogous complexes with neutral adenosine [22]. Thus, the results from the spectrophotometric titrations indicate that although the stability constant of $H_2LZn_2^{6+}$ is not very large and its formation requires a large excess of Zn(II) ions, significant amounts of this species must be formed under the synthetic conditions and its expected lower solubility with respect to H_2L^{2+} and H_2LZn^{4+} can be the responsible of its isolation.

When taken together with the potentiometric results, the spectrophotometric data indicate that protonation of L to the H_2L^{2+} form causes a change in the co-ordination mode of the ligand in such a way that there is now a single monodentate interaction of the Zn(II) ions with the N(7) atoms. In contrast, the less protonated ligand species L and HL^+ interact more strongly with the metal ions, which suggests again the use of additional donor sites.

Another interesting aspect to consider in the interpretation of the equilibrium data is that L is symmetrical and contains two equivalent adenine fragments. For the interaction with both H^+ and Zn^{2+} there are always two equivalent sites that may behave independently or show some kind of co-operative behaviour. For statistical reasons, the quotient between successive equilibrium constants must be 4 if the adenines behave independently, whereas a co-operative behaviour would lead to a significantly smaller value of the quotient. In contrast, if there is some destabilisation associated to the electrostatic repulsion caused by the existence of two H^+ (or two Zn^{2+}) ions close to each other, the value of the second equilibrium constant will decrease and the quotient K_1/K_2 will be significantly higher than 4. The experimental data indicate that the quotient K_{H1}/K_{H2} is 11.7, whereas K_{M1}/K_{M2} is 10.0 for co-ordination of the Zn(II) ions to L, 5.0 for co-ordination to HL^+ and 2.5 ($ZnCl_2$ solutions) or 6.3 ($ZnSO_4$ solutions) for the interaction with the H_2L^{2+} species; all these values are not very far from the statistical prediction and indicate that the adenine sub-units in L behave almost independently, at least in acidic solutions.

4. Conclusion

The spectrophotometric equilibrium studies indicate that the $H_2LZn_2^{6+}$ species, isolated as $[H_2L(ZnCl_3)_2]\cdot 2H_2O$ (**4**), is formed in strongly acidic solutions according to the model shown in Fig. 5. The crystal structure of the outer-sphere $(H_2L)[HgCl_4]\cdot 3H_2O$ complex (**3**) shows that N(1) and N(1′) are the protonation sites of the ligand. Moreover, the crystal structure of **4** also indicates that the adeninium moieties are formed by means of protonation at the N(1) sites and metal co-ordination at both N(7) atoms. The N(9) sites of the adeninium fragments are free of any interaction with the metal ions.

As the spectrophotometric data indicate that the stability of species with a single interaction between Zn(II) and the N(7) of the adenine fragments in L is similar to that of the Zn(II)-adenine complexes, the formation of a LZn^{2+} species with that kind of interaction should lead to a log β value smaller than ca. 2, which is far from the value (4.2) derived from the analysis of the potentiometric data. These findings strongly suggest that a change in the pH of the solution causes important changes in the co-ordination behaviour of L, probably in the sense of favouring polydentate interactions with the metal ion at higher pH. Further work is required to gain insight into this behaviour and to obtain a better understanding of the reasons that lead to the rich solution chemistry shown by L in contrast to our previous results using bis(adenines) linked through the N(9) atoms, for which only outer sphere complexes without any specific interaction of the adenines with the metal ion were found.

5. Supplementary material

Crystallographic data are available from the Cambridge Crystallographic Data Centre, 12 Union Road, Cambridge CB2 1EZ, UK (fax: +44-1223-336033; e-mail: deposit@ccdc.cam.ac.uk or www: http://www.ccdc.cam.ac.uk) on request, quoting the deposition number 175813 for **3** and 175812 for **4**.

Acknowledgements

We acknowledge financial support from the Spanish DGICYT (PB98-0123 and BQ2000-0232).

References

[1] R.W. Gellert, R. Bau, in: H. Sigel (Ed.), Metal Ions in Biological Systems, Vol. 8, Marcel Dekker, New York, 1979, pp. 1–55.
[2] R.B. Martin, Y.H. Mariam, in: H. Sigel (Ed.), Metal Ions in Biological Systems, Vol. 8, Marcel Dekker, New York, 1979, pp. 57–124.
[3] D.J. Hodgson, Prog. Inorg. Chem. 23 (1977) 211–254.
[4] D.T. Browne, J. Eisinger, N.J. Leonard, J. Am. Chem. Soc 90 (1968) 7302–7323.
[5] B.L. Vallee, in: H. Gray, I. Bertini (Eds.), Zinc Enzymes, Birkhauser, Boston, MA, 1986, pp. 1–16.
[6] J.K. Barton, S.J. Lippard, in: T.G. Spiro (Ed.), Nucleic Acid-Metal Ion Interactions, Wiley, New York, 1980, pp. 31–113.
[7] A. García-Raso, J.J. Fiol, F. Bádenas, X. Solans, M. Font-Bardia, Polyhedron 18 (1999) 765–772.
[8] A. García-Raso, J.J. Fiol, F. Bádenas, X. Solans, M. Font-Bardia, Polyhedron 18 (1999) 3077–3083.
[9] M. Malon, Z. Travnicek, M. Marysko, R. Zboril, M. Maslan, J. Marek, K. Dolezal, J. Rolcik, V. Krystof, M. Strnad, Inorg. Chim. Acta 323 (2001) 119–129.
[10] Z. Travnicek, M. Malon, Z. Sindelar, K. Dolezal, J. Rolcik, V. Krystof, M. Strnad, J. Marek, J. Inorg. Biochem. 84 (2001) 23–32.
[11] B.L. Heyl, K. Shinozuka, S.K. Miller, D.G. Vanderveer, L.G. Marzilli, Inorg. Chem. 24 (1985) 661–666.
[12] J.H. Lister, J. Chem. Soc. (1960) 3682–3684.
[13] G.M. Sheldrick, Acta Crystallogr. Sect. A 46 (1990) 467–473.
[14] G.M. Sheldrick, A Computer Program for Determination of Crystal Structure, University of Göttingen, Germany, 1994.
[15] International Tables of X-Ray Cristallography, Vol. IV, Kynoch Press, Birmingham, UK, 1974, pp. 99–100 and 149.
[16] A.E. Martell, R.J. Motekaitis, in: Determination and Use of Stability Constants, VCH, New York, 1992.
[17] R.M. Smith, A.E. Martell, R.J. Motekaitis, in: NIST Critical Stability Constants of Metal Complexes Database, US Department of Commerce, Gaithesbourgh, 1993.
[18] K.A. Connors, in: Binding Constants. The Measurement of Molecular Complex Stability, Wiley, New York, 1987, pp. 139–168.
[19] M.J. Olivier, A.L. Beauchamp, Inorg. Chem. 19 (1980) 1064–1067.
[20] M.J. Olivier, A.L. Beauchamp, Acta Crystallogr. Sect. B 38 (1982) 2159–2164.
[21] F. Zamora, M. Sabat, B. Lippert, Inorg. Chim. Acta 267 (1998) 87–91.
[22] H. Lönnberg, in: K. Burger (Ed.), Biocoordination Chemistry. Coordination Equilibria in Biologically Active Systems, Ellis Horwood, London, 1990, pp. 284–328.
[23] M. Taylor, Acta Crystallogr. B29 (1973) 884–890.
[24] M. McCall, M.R. Taylor, Biochim. Biophys. Acta 390 (1975) 137–139.
[25] J. Maixner, J. Zachová, Acta Crystallogr. Sect. C 49 (1993) 927–929.
[26] M. McCall, M.R. Taylor, Acta Crystallogr. Sect. B 32 (1976) 1687–1691.
[27] P.T. Muthiah, S.K. Mazumdar, S. Chaudhuri, J. Inorg. Biochem. 19 (1983) 237–246.
[28] K. Nakamoto, in: Infrared and Raman Spectra of Inorganic and Coordination Compounds, Wiley, New York, 1978.
[29] R. Savoie, J.-J. Jutier, L. Prizant, A.L. Beauchamp, Spectrochim. Acta A38 (1982) 561–568.
[30] M. Tsuboi, S. Takahasha, I. Harada, in: J. Duchesne (Ed.), Physiochemical Properties of Nucleic Acids, Vol. 2, Academic Press, London, 1973, p. 113 and 119.
[31] R.M. Izatt, J.J. Christensen, J.H. Rytting, Chem. Rev. 71 (1971) 439–481.
[32] R. Tauler, M.J.A. Rainer, B.M. Rode, Inorg. Chim. Acta 123 (1986) 75–82.
[33] G. Mukherjee, T. Ghosh, J. Inorg. Biochem. 59 (1995) 827–833.
[34] K. Ramalingam, C.R. Krishnamoorthy, Inorg. Chim. Acta 67 (1982) 167–172.
[35] R.B. Martin, Acc. Chem. Res. 18 (1985) 32–38.
[36] H. Sigel, N.A. Corfù, L. Ji, R.B. Martin, Comments Inorg. Chem. 13 (1992) 35–59.
[37] P. De Meester, A.C. Skapski, J. Chem. Soc., Dalton Trans. (1972) 2400–2404.
[38] X. Zhu, E. Rusanov, R. Kluge, H. Schmidt, D. Steinborn, Inorg. Chem. 41 (2002) 2667–2671.
[39] E. Szlyk, I. Lakomska, Polyhedron 11 (1992) 3147–3153.
[40] E. Bugella-Altamirano, D. Choquesillo-Lazarte, J. M. González-Pérez, M. J. Sánchez-Moreno, R. Martin-Sánchez, J. D. Martín-Ramos, B. Covelo, R. Carballo, A. Castiñeiras, J. Niclós-Gutiérrez, Inorg. Chim. Acta (2002) in press.